STUDY ON SEEPAGE CHARACTERISTICS OF CROSS FRACTURES IN ADJACENT AND CONVECTIVE FLOW MODES

by

Zun-Dong YANG[a,b], Zhao LIU[c*], Jing XIE[a,b], Rui-Feng TANG[a,b], and Xiao-Bin GU[d]

[a]College of Water Resource and Hydropower, Sichuan University, Chengdu, China
[b]State Key Laboratory of Hydraulics and Mountain River Engineering, Sichuan University, Chengdu, China
[c]Zhensha Hydropower Construction Management Branch, GuonengDadu River Basin Hydropower Development Co., Ltd. Leshan, Sichuan, China
[d]JinshiDrilltech Co. Ltd., Tangshan, China

Original scientific paper
https://doi.org/10.2298/TSCI220828013Y

The distribution of fractures in the underground rock mass is complex, so it is of great significance to study the parameter characteristics of fracture seepage for geothermal exploitation, land subsidence, and other fields. Based on the Weierstrass-Mandelbrot function, several X-shaped fracture models with different roughness are established, and the fracture seepage law under different roughness and inlet pressure is studied. At the same time, the center (cross-region) of the X-shaped fracture is selected as the research object, and the seepage difference characteristics of the cross-region under the two inlet modes of adjacent flow and convective flow are compared and analyzed. The results show that the outlet velocity of fracture fluid is inversely proportional to the fractal dimension and is directly proportional to the inlet pressure.

Key words*: X-shaped fracture, fracture seepage, fractal dimension, cross-region, adjacent and convective flow*

Introduction

In recent years, fracture seepage has become a research hotspot in academia. It has been applied in the fields of natural gas and oil exploitation [1], geothermal exploitation [2-4], coal mining [5, 6] and extraction of coal bed methane [7, 8], land subsidence [9], induced earthquakes [10, 11], disposal of nuclear waste and pollutants [12, 13], *etc*. Nowadays, the profound evolution of the international situation and the turbulent global energy supply and demand pattern have forced mining to go deeper [14-19], the research on the seepage law of cracks in rocks and coal seams has become more and more important. According to a large number of statistics, the basic units of underground medium fractures are divided into single fractures and cross fractures.

*Corresponding author, e-mail: 504797414@qq.com

Scholars have done a lot of research on rock fracture seepage based on the aforementioned two basic fracture elements. Liu *et al.* [20] studied the effects of different fractal dimensions, fracture width, and inlet pressure on fracture flow characteristics by numerical simulation of a single fracture. Zhao *et al.* [21] conducted numerical simulation of single-phase laminar flow and studied the seepage characteristics of single fracture in different projection directions. Xie*et al.* [22] combined with 3-D printing technology to establish solid cross-fracture models with different fractal dimensions, quantitatively evaluated and discussed the pressure drop loss and competitive diversion behavior of two fractures with different fractal dimensions. Tang *et al.* [23] selected the *Y*-shaped fracture as the research object, carried out numerical simulation research on it, and analyzed the essence of fracture competitive diversion from the perspective of fluid streamline. Ma *et al.* [24] developed discontinuous Galerkin and continuous Galerkin methods for compressible single-phase and two-phase flows in porous media, and the flow behavior of single-phase and two-phase fluids in fractured porous media were predicted. Liu *et al.* [25] studied a series of non-linear flow behaviors of fluid passing through the intersection of fractures by numerical simulation of discrete fracture elements. However, for the cross fractures in the underground rock mass fracture network, its inflow modes are usually very complex. For example, the fluid in the underground medium can flow into the fracture from two adjacent fracture inlets, or from both ends of a fracture branch. The different inflow modes will have a significant impact on the fluid seepage characteristics in the cross fractures, which still needs to be discussed in depth.

In this study, the Weierstrass-Mandelbrot function is used to construct *X*-shaped fractures, and two inflow modes are selected to study the changes of seepage characteristics of *X*-shaped fractures with different fractal dimensions and different inlet pressures. Combined with the numerical simulation software, four fracture conditions with five pressure conditions in each condition are established, and the behavior of convective flow and concentration in the *X*-shaped fracture cross-region is mainly discussed. The research results can provide new insights for evaluating the fluid flow behavior of underground fracture network.

Model building

In this paper, the *X*-shaped fracture which is often found in the geological community is used as the starting point, and four working conditions are set up (the fractal dimensions of the two fractures are the same as 1.0, 1.1, 1.2, 1.3.). For the inlet of each working condition, a total of five pressure conditions are set: 50 Pa, 100 Pa, 150 Pa, 200 Pa, and 250 Pa, and the outlet pressure is 0. The intersection angle of the cross fracture is maintained at 90° , the fracture average aperture and straight length are set as 0.5 mm and 100 mm. As for the selection of inlet, there are two cases: adjacent and convective flow, as shown in fig. 1(a)-1(c), and where each cross-section of the *X*-fracture is marked, as shown in fig. 1(d).

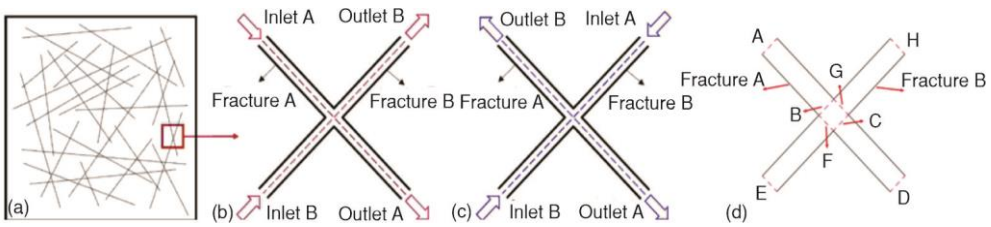

Figure 1. Two inflow modes: adjacent and convective flow; (a) discrete fracture network, (b) adjacent flow, (c) convective flow, and (d) labeling of each cross section of the *X*-fracture

The Weierstrass-Mandelbrot function is expressed as [20, 22]:

$$W(t) = \sum_{n=-\infty}^{\infty} (1 - e^{ib^n t}) e^{i\varphi_n} / b^{(2-D)n} \tag{1}$$

where b is a real number greater than 1, which reflects the degree of deviation of the curve from the straight line, φ_n is any phase angle and $D \in (1,2)$ is the fractal dimension. Selecting the real part of function $W(t)$ (cosine function) as the fractal function can get the following expression:

$$C(t) = \mathrm{Re}W(t) = \sum_{n=-\infty}^{\infty} (1 - \cos b^n t) / b^{(2-D)n} \tag{2}$$

It is well known that it is a continuous, in derivable fractal curve with fractal dimension D, in which the fractal dimension satisfies the following relationship:

$$D_{HB} - \left(\frac{B}{b}\right) \le D \le D_{HB} \tag{3}$$

where B is a constant and D_{HB} is the Hausdorff-Besicovitch dimension. Take $B = 1.4$ in fractal unction $C(t)$, and MATLAB is used to generate fractal curves to construct the X-fracture model under four working conditions, as shown in fig. 2.

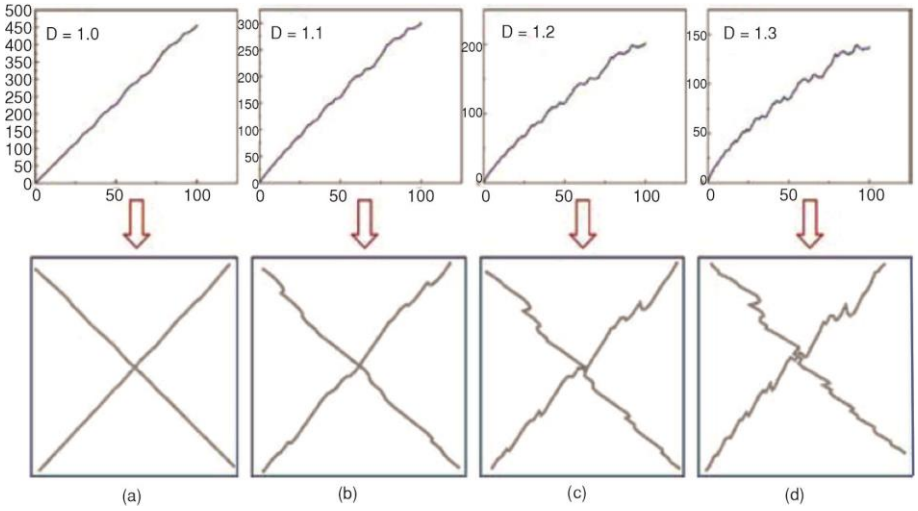

Figure 2. The *X*-fracture model based on fractal function; (a) Pattern 1, (b) Pattern 2, (c) Pattern 3, and (d) Pattern 4

The COMSOL Multiphysics 6.0 software was used to conduct numerical simulation of all working involved conditions, and the density and dynamic viscosity of the fluid were set to $1 \cdot 10^3$ kg/m^3 and $1.01 \cdot 10^{-3}$ Pa·s.

Result and discussion

Analysis of fracture seepage characteristic parameters with different roughness

According to the numerical simulation results, the relationship between fracture seepage velocity and inlet pressure and fracture fractal dimension under the conditions of adjacent flow and convection is discussed.

In the adjacent flow and convection mode, the seepage characteristic curve is shown in fig. 3. It is not difficult to find that when the inlet pressure is constant, with the increase of fractal dimension, the roughness of the fracture also increases, and the fluid average velocity of the seepage outlet section of the fracture shows a downward trend. Moreover, with the increase of pressure, the gap of fracture outlet velocity with different fractal dimensions is also increasing. This means that when the fracture roughness increases, the direction change increases the seepage length of the fluid, when the fluid-flows into the fracture with large roughness, the more energy it consumes, and the less speed it flows out of the fracture. When the fractal dimension of the crack is fixed, the average velocity of the fluid at the crack outlet increases linearly with the increase of the inlet pressure, which indicates that the increase of the inlet pressure also represents the increase of the energy of the water flow, the velocity of the fluid is larger.

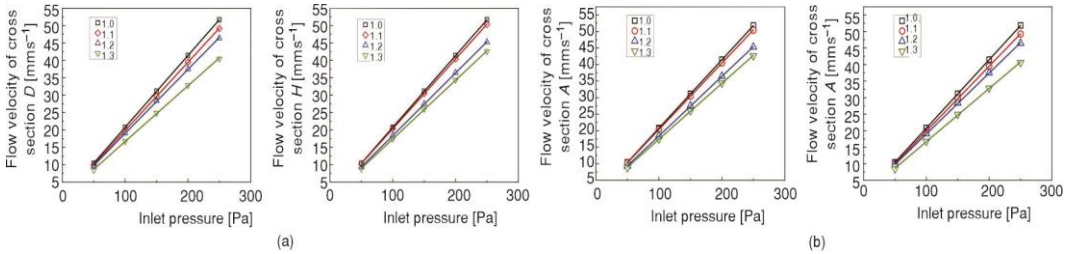

Figure 3. Flow velocity at crack outlet under adjacent and convection flow mode; (a) flow velocity of cross section D and H in adjacent flow and (b) flow velocity of cross section A and D in convective flow

Analysis of seepage characteristics in the intersection region under adjacent and convective flow modes

The region formed with sections B, C, F and G as the boundaries is defined as the intersection region. In the adjacent and convective flow mode, due to the complex seepage

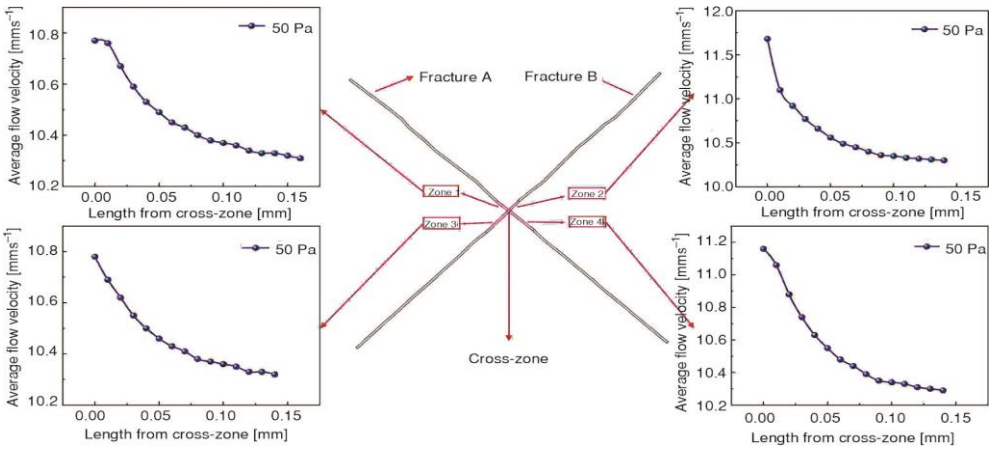

Figure 4. Schematic diagram of the influence of the intersection region on the four branch fractures (fractal dimension is 1.0, the inlet pressure is 50 Pa, and the inlet mode is adjacent flow)

behavior of the fluid in the cross-region, a series of kinematic behaviors such as confluence and opposite impact will occur after the fluid-flows into the cross-region, which will lead to sharp changes in the fluid velocity in the cross-region and spread to the four branch fractures

with the cross-region as the center, a range area affected by the cross-region is formed, which is divided into four parts (Zone 1, Zone 2, Zone 3, Zone 4), as shown in fig. 4. Taking the fractal dimension of the fracture as 1.0, the inlet pressure as 50 Pa and the inflow mode as the adjacent flow as an example, the relationship between the average velocity of the fluid near the cross-region and the distance from the cross-region is drawn.

Velocity gradient is the change rate of fluid velocity. It is usually used as one of the important indicators to evaluate whether a place is a potential animal habitat, which affects the foraging of fish and the selection of breeding sites. At the same time, it can also be used to describe the spatial change of velocity to characterize the complexity of water flow [26-28]. There is the relation:

$$grad(v) = \frac{V_2 - V_1}{L} \tag{4}$$

where V_1 and V_2 are the average velocity of cross-section 1 and cross-section 2, respectively, $V_2 > V_1$, and L is the distance between cross-section 1 and cross-section 2.

For the adjacent flow mode, Zone 1 and Zone 3 are the areas where the fluid-flows when it is about to flow into the cross-region (upstream area), and Zone 2 and Zone 4 are the areas where the fluid-flows when it leaves the cross-region (downstream area). From the cross-region to the four branches, calculate the flow velocity gradient when the fluid approaches the cross-region, as shown in fig. 5. It can be seen from the figure that for Patterns 1, 2, and 4, when the fluid is about to enter the cross-region, its velocity increases slowly with the increase of inlet pressure. After flowing out of the cross-region, the fluid speed decreases rapidly, and the decline speed is about five times the growth speed when the fluid enters the cross-region. As for Pattern 3, the change of velocity gradient is more complex due to the short distance of the first straight line that spreads around the cross-region, fig. 6, and its change law with inlet pressure is different from that of the other three Patterns. But on the whole, it can still be seen that the velocity gradient in the upstream area is smaller than that in the downstream area under various pressures, and with the increase of inlet pressure, the growth rate of velocity gradient in the upstream area is smaller than that in the downstream area. In the convective mode, the variation of velocity gradient with inlet pressure under different conditions is similar to that of adjacent flow, which will not be repeated here.

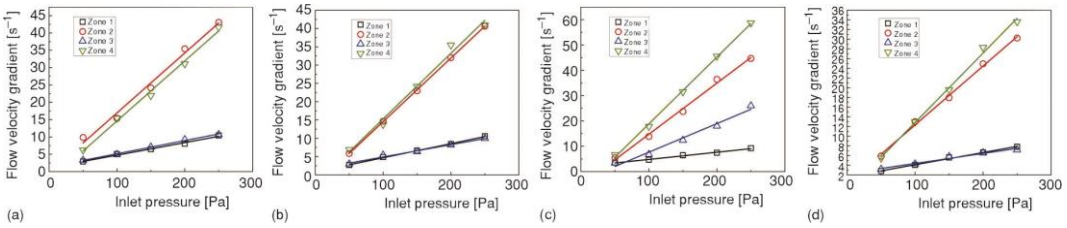

Figure 5. Flow velocity gradient vs inlet pressure of adjacent flow; (a) Pattern 1, (b) Pattern 2, (c) Pattern 3, and (d) Pattern 4

Cloud analysis of cross-region seepage parameters in adjacent and convective flow modes

In order to deeply explore the difference of seepage characteristics in the cross-region under adjacent and convective flow mode, take the *X*-fracture with fractal dimension of 1.0 and inlet pressure of 50 Pa as an example, the velocity contours are drawn, as

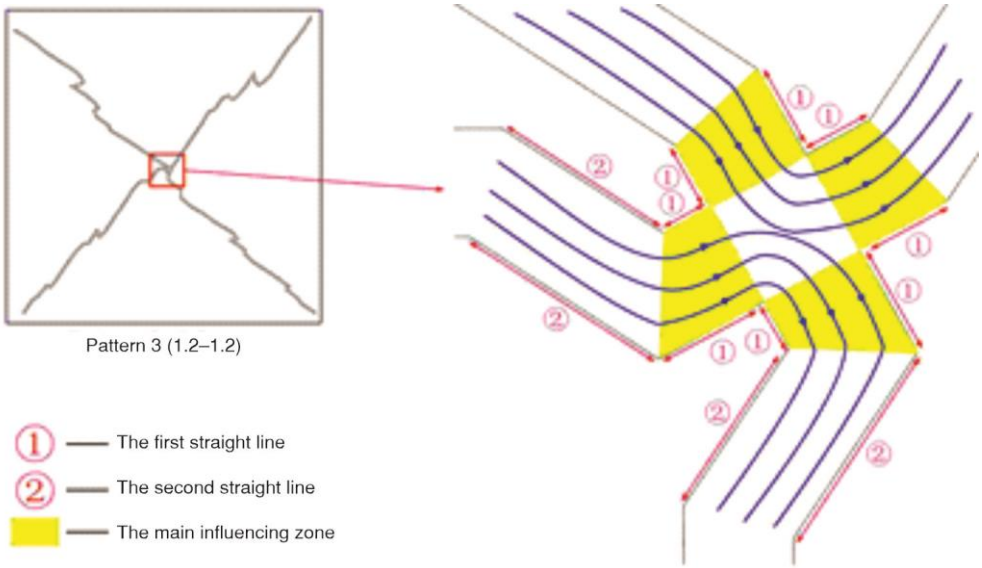

Figure 6. Partial enlargement of cross-region under Pattern 3

shown in fig. 7(a). It can be seen that in the convective mode, a low-velocity region similar to a square is formed in the cross-region of its *X*-fracture, and in this low-velocity region, the fluid velocity increases linearly around the equal spacing, forming a multi-layer annular velocity contour. Take the *X*-fracture with fractal dimension of 1.0 and inlet pressure of 50 Pa as an example, the streamline diagram of the cross-region is drawn. It can be seen from fig. 8(a) that when the fluid-flows in the form of convection, the fluid flowing in the opposite direction in the cross-region will collide, resulting in kinetic energy loss. After the collision, the kinetic energy of the two branches of the fluid will be redistributed and flow out of the cross-region at residual velocity, respectively. The greater the velocity of the fluid, the greater the kinetic energy loss, the smaller the kinetic energy after the collision, the smaller the residual velocity. It can be seen that the kinetic energy loss of the fluid in the center of the cross-region is the largest, and its residual velocity is also the smallest. When the fluid diffuses from the center of the cross-region to the surrounding area, the kinetic energy loss of the fluid is smaller than that of the center area because its velocity before the collision is not as large as that of the center, and its residual velocity after the collision is also larger than that of the center area, the impact of the fluid on the opposite direction is also smaller. Therefore, the velocity distribution of the fluid takes the center of the cross-region as the origin and spreads around, forming a multi-layer annular velocity cloud.

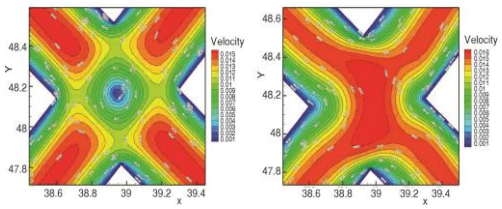

Figure 7. Velocity contours in convective and adjacent flow mode (Pattern 1-50Pa); (a) convective flow and (b)adjacent flow

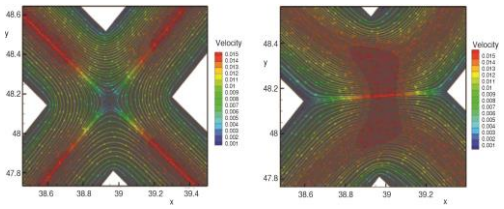

Figure 8. Streamlines in convective and adjacent flow mode (Pattern 1-50Pa); (a) convective flow and (b) adjacent flow

In the adjacent flow mode, the flow line diagram of the cross-region is drawn when the fractal dimension is 1.0 and the inlet pressure is 50 Pa, as shown in fig. 8(b). It can be seen that when the fluid of the two inlet branches of the *X*-fracture flow into the cross-region, for the upper half of the *X*-fracture, the fluid flow direction is the left inlet branch flows in and the right outlet branch flows out, and the flow line forms a concave arc shape. For the lower part of *X*-fracture, similarly, the fluid streamline forms a convex arc shape. When the fluids at the two inlets enter the cross-region, the upper and lower fluids intersect, especially the upper and lower arc-shaped parts with the largest curvature intersect the most strongly, that is, the central part of the X-shaped fracture cross-region. The straight line connecting the left and right endpoints of the cross-region is defined as straight line N, and the midpoint O of the line N is the point where the upper and lower fluids intersect most violently, the fluid velocity is the largest and the kinetic energy is the largest. Taking this as the center point, it spreads around, a saddle-shaped high-speed area is formed. Taking point O as the center point, which spreads to both sides of the straight line N, the fluid velocity gradually decreases to the minimum at the left and right endpoints, this is because the intersection intensity of the fluid gradually weakens from the O point to the left and right sides, so that the increase of the kinetic energy of the fluid gradually decreases, and the velocity also gradually decreases.

Conclusion

Based on the *X*-fracture constructed by the Weierstrass-Mandelbrot function, the numerical simulation study of different inlet pressures and different fractal dimensions in adjacent flow and convection modes was carried out, and the seepage characteristic parameters of the fracture fluid were analyzed. In the convective and adjacent flow modes, the outlet velocity of the fracture fluid is inversely proportional to the fractal dimension and proportional to the inlet pressure. In the vicinity of the cross-region, the influence of the cross-region on the upstream fluid is smaller than that on the downstream fluid. With the increase of the inlet pressure, the velocity in the upstream area increases slowly, and the velocity in the downstream area decreases rapidly. In the adjacent flow mode, the intersection area has a weak influence on the upstream fluid and a strong influence on the downstream fluid. The flow velocity gradient in the downstream area is 5 times that of the upstream area, and the same is true in the convection mode.In the convective flow mode, the fluids collide in the opposite flow in the cross-region, forming a multi-layer annular low-velocity area in the cross-region; in the adjacent flow mode, when the fluid enters the cross-region, two fluids converge, and a saddle-shaped high-speed zone is formed.

Acknowledgment

This work was financially supported by National Natural Science Foundation of China (52004167, 52225403)and the Applied Basic Research Programs of Sichuan Province (No.2021YJ0411).

Nomenclature

D – fractal dimension, [–]
$grad(v)$ – velocity gradient, [s^{-1}]
L – distance, [mm]
V – average velocity, [mms^{-1}]

Greek symbol

φ_n – any phase angle, [°]

References

[1] Gao, C., *et al.*, Coupling Between the Statistical Damage Model and Permeability Variation in Reservoir Sandstone: Theoretical Analysis and Verification, *Journal of Natural Gas Science and Engineering*, *37* (2017), Jan., pp. 375-385
[2] Dragović, N. M., *et al.*, Potentialsand Prospectsfor Implementationof Renewable Energy Sourcesin Serbia, *Thermal Science*, *23* (2019), 5B, pp. 2895-2907
[3] Lepillier, B., *et al.*, A Fracture Flow Permeability and Stress Dependency Simulation Applied to Multi-reservoirs, Multi-production Scenarios Analysis, *Geothermal Energy*, *7* (2019), Dec., 1
[4] Luo, C., *et al.*, The Case Studyof Binary Power Plant Basedon Thermoeconomicsin Sichuan, China, *Thermal Science*, *22* (2018), 2, pp. 1003-1014
[5] Gao, M., *et al.*, In-situ Disturbed Mechanical Behavior of Deep Coal Rock (in Chinese), *Journal of China Coal Society*,*45* (2020), 08, pp. 2691-2703
[6] Gao, M., *et al.*, The Location Optimum and Permeability-Enhancing Effect of a Low-Level Shield Rock Roadway, *Rock Mechanics and Rock Engineering*, *51* (2018), 9, pp. 2935-2948
[7] Gao, M., *et al.*, Fractal Evolution and Connectivity Characteristics of Mining-induced Crack Networks in Coal Masses at Different Depths, *Geomechanics and Geophysics for Geo-Energy and Geo-Resources*, *7* (2021), Feb., 1
[8] Li, Q., *et al.*, Effects of Natural Micro-fracture Morphology, Temperature and Pressure on Fluid Flow in Coals Through Fractal Theory Combined with Lattice Boltzmann Method, *Fuel*, *286* (2021), Part 2, 119468
[9] Preisig, G., *et al.*, Modelling Discharge Rates and Ground Settlement Induced by Tunnel Excavation, *Rock Mechanics and Rock Engineering*, *47* (2014), 3, pp. 869-884
[10] Brantut, N., Dilatancy-induced Fluid Pressure Drop During Dynamic Rupture: Direct Experimental Evidence and Eonsequences for Earthquake Dynamics, *Earth and Planetary Science Letters*, *538* (2020), May, 116179
[11] Castro, A. F. P., *et al.*, Stress Chatter via Fluid Flow and Fault Slip in a Hydraulic Fracturing-Induced Earthquake Sequence in the Montney Formation, British Columbia, *Geophysical Research Letters*, *47* (2020), July, 14
[12] Bai, B., *et al.*, An Experimental and Theoretical Study of the Seepage Migration of Suspended Particles with Different Sizes, *Hydrogeology Journal*, *24* (2016), 8, pp. 2063-2078
[13] Wu, Q.,J. Wang, A Thermo-Hydro-Mechanical Coupling Analysis for the Contaminant Transport in a Bentonite Barrier with Variable Saturation, *Water*, *12* (2020), 11, 3114
[14] [Gao, M., *et al.*, Mechanical Behavior of Coal Under Different Mining Rates: A Case Study from Laboratory Experiments to Field Testing, *International Journal of Mining Science and Technology*, *31* (2021), 5, pp. 825-841
[15] Mingzhong, G., *et al.*, Discing Behavior and Mechanism of Cores Extracted from Songke-2 Well at Depths Below 4,500 m, *International Journal of Rock Mechanics and Mining Sciences*, *149* (2022), Jan., 104976
[16] Yang, B.-G., *et al.*, Exploration of Weakening Mechanism of Uniaxial Compressive Strength of Deep Sandstone Under Microwave Irradiation, *Journal of Central South University*, *29* (2022), 2, pp. 611-623
[17] Gao, M., *et al.*, The Novel Idea and Technical Progress of Lunar In-situ Condition Preserved Coring, *Geomechanics and Geophysics for Geo-Energy and Geo-Resources*, *8* (2022), Apr., 2
[18] Gao, M.-Z., *et al.*, The Mechanism of Microwave Rock Breaking and Its Potential Application to Rock-Breaking Technology in Drilling, *Petroleum Science*, *19* (2022), 3, pp. 1110-1124
[19] Gao, M.-z., *et al.*, Calculating Changes in Fractal Dimension of Surface Cracks to Quantify How the Dynamic Loading Rate Affects Rock Failure in Deep Mining, *Journal of Central South University*, *27* (2020), 10, pp. 3013-3024
[20] Liu, J.-J., *et al.*, Flow Characteristics of Fractal Fracture With Different Fractal Dimension and Different Fracture Width, *Thermal Science*, *25* (2021), 6B, pp. 4477-4484
[21] Zhao, Z., Zhou, X.-P., Digital Voxel-based Fracture Extraction: Insights to Characterization of Single Fracture Flow and Anisotropy Permeability, *Journal of Natural Gas Science and Engineering*, *84* (2020), Dec., 103635
[22] Xie, J., *et al.*, Fluid Flow Characteristics of Cross-fractures With Two Branch Fractures of Different Roughness Controlled by Fractal Dimension: An Experimental Study, *Journal of Petroleum Science and Engineering*, *196* (2021), Jan., 107996

[23] Tang, R., *et al.*, Research on Seepage Characteristics of Y-Shaped Fractures under Different Fracture Roughness, *Geofluids*, *2022* (2022), ID7521955
[24] Ma, T., *et al.*, Discontinuous and Continuous Galerkin Methods for Compressible Single-phase and Two-phase Flow in Fractured Porous Media, *Advances in Water Resources*, *156* (2021), Oct., 104039
[25] Liu, R., *et al.*, Critical Hydraulic Gradient for Nonlinear Flow Through Rock Fracture Networks: The Roles of Aperture, Surface Roughness, and Number of Intersections, *Advances in Water Resources*, *88* (2016), Feb., pp. 53-65
[26] Crowder, D. W., *et al.*, Vorticity and Circulation: Spatial Metrics for Evaluating Flow Complexity in Stream Habitats, *Canadian Journal of Fisheries and Aquatic Sciences*, *59* (2002), 4, pp. 633-645
[27] Yang, X. J., An Insight on the Fractal Power Law Flow: from a Hausdorff Vector Calculus Perspective, *Fractals*, *30* (2022), 3, pp. 2250054-929
[28] Yang, X. J., The Vector Power-Law Calculus with Applications in Power-Law Fluid Flow, *Thermal Science*, *24* (2020), 6B, pp. 4289-4302

Paper submitted: August 28, 2022
Paper revised: November 18, 2022
Paper accepted: November 22, 2022